

This document was prepared in conjunction with work accomplished under Contract No. DE-DE-AC09-76SR00001 with the U.S. Department of Energy.

#### DISCLAIMER

This report was prepared as an account of work sponsored by an agency of the United States Government. Neither the United States Government nor any agency thereof, nor any of their employees, makes any warranty, express or implied, or assumes any legal liability or responsibility for the accuracy, completeness, or usefulness of any information, apparatus, product or process disclosed, or represents that its use would not infringe privately owned rights. Reference herein to any specific commercial product, process or service by trade name, trademark, manufacturer, or otherwise does not necessarily constitute or imply its endorsement, recommendation, or favoring by the United States Government or any agency thereof. The views and opinions of authors expressed herein do not necessarily state or reflect those of the United States Government or any agency thereof.

This report has been reproduced directly from the best available copy.

Available for sale to the public, in paper, from: U.S. Department of Commerce, National Technical Information Service, 5285 Port Royal Road, Springfield, VA 22161  
phone: (800) 553-6847  
fax: (703) 605-6900  
email: [orders@ntis.fedworld.gov](mailto:orders@ntis.fedworld.gov)  
online ordering: <http://www.ntis.gov/support/index.html>

Available electronically at <http://www.osti.gov/bridge>

Available for a processing fee to U.S. Department of Energy and its contractors, in paper, from: U.S. Department of Energy, Office of Scientific and Technical Information, P.O. Box 62, Oak Ridge, TN 37831-0062  
phone: (865)576-8401  
fax: (865)576-5728  
email: [reports@adonis.osti.gov](mailto:reports@adonis.osti.gov)

DISTRIBUTION:

J. W. Croach -	R. J. Pryor
A. A. Johnson, Wilm.	C. J. Temple
C. H. Ice -	S. D. Harris
L. H. Meyer, SRL	J. P. Morin
J. R. Hilley	D. R. Muhlbaier
P. L. Roggenkamp	<u>TIS Copy</u>
M. M. Anderson	Vital Records File
W. R. Graves	

February 18, 1976

M E M O R A N D U M

TO: G. F. MERZ

FROM: D. I. ORLOFF\*-D. R. MUHLBAIER *JEM*

TIS FILE  
RECORD COPY

STEAM VOID BEHAVIOR AND POSTULATED MATHEMATICAL MODEL  
FOR RHTF STUDIES

INTRODUCTION

In the event of postulated but unlikely nuclear accidents, steam could be discharged into the bulk moderator space of SRP reactors. Characterization of the behavior of the steam is necessary to permit calculation of the course of the transient. Studies are being conducted in the Reactor Hydraulic Test Facility (RHTF) to determine the behavior of steam in subcooled water and to develop mathematical models describing the behavior. This memorandum describes recent experimental results and presents an analytical model used in correlating the data.

SUMMARY

Newly designed needle point resistivity probes have been used to show that two-phase slug flow occurs in the bulk moderator space during steam injection from a uniform lattice mockup with clusters of steaming assemblies. Techniques have been developed to measure slug frequency, vertical and horizontal dimensions,

\* Faculty Research Participant, University of South Carolina

and vertical velocity.

Analytical study indicates that both direct vapor-liquid interface heat transfer and film condensation heat transfer (to tube walls) are responsible for vapor slug condensation. Derived equations can be used with future experimental data to determine a Nusselt number correlation for direct vapor-liquid interface condensation heat transfer. This correlation can then be used to compute the vapor slug size as a function of vertical position in the tank.

## DISCUSSION

### Test Conditions and Results

Tests were conducted in the RHTF to determine the behavior of steam discharged from mockup assemblies into the subcooled water of the bulk moderator space.

Earlier tests<sup>1</sup> measured the total steam volume and average void fraction within the bulk moderator space for various conditions. The present testing is directed toward detailed study of the steaming process and identification of local instantaneous conditions (non-time averaged) for the purpose of determining controlling mechanism. This includes determining which of the four major regimes of two-phase flow (Figure 1) occur.<sup>2</sup>

The RHTF<sup>3</sup> is a 1/4-scale reactor model (Figure 2). Tests were conducted by injecting 10,000 #/hr. of steam into the central 18 assemblies (uniform lattice) and discharging 3,000 or 5,000 gpm water from the other 168 assemblies (Figure 3). The water temperature was varied to change the subcooling and resultant void size and steam quenching rate.

Previous studies<sup>4</sup> for single-phase liquid showed vertical upflow at the center of the tank (Figure 4) which could be expected for the uniform lattice steaming configuration in the center of the tank. The one-dimensional flow offered the possibility of measuring the steam-liquid interface velocity. Fast response needle point resistivity probes were fabricated and assembled in vertical and horizontal arrays as shown in Figures 5 and 6. Small bare tip thermocouples were included in the probe array and were designed to measure ~90% of a step change in 30 msec. Resistivity probes produce a signal change at the passage of a vapor-liquid interface. Recording of the response between two or more probes enables measurement of lag time which could be related to the bubble interface velocity.

Initial tests were conducted with the vertical probe placed at the approximate center of the RHTF and 18 inches above the tank bottom (Figure 7). Typical resistivity vs time traces as recorded on the oscillograph from each of the three needles making up the probe are shown in Figure 8. (Steam caused the

signal to change but the relative amplitude has no significant meaning and cannot be compared between signals.) Trace No. 1 was obtained from the needle nearest the tank bottom, trace No. 2 from the middle probe, and trace No. 3 from the top probe. Observations from this and similar traces indicate: 1) the resistivity signal has a very regular frequency which is typical of the slug flow regime, and 2) comparison of signals 1, 2, and 3 show a decrease in vapor slug duration as the vapor slug traverses the three needles. Condensation reduces the vapor slug volume and height as the slug rises and cause the reduced duration.

The signals depicted in Figure 8 were analyzed over a period of six seconds for statistical variation in frequency. A plot of normalized slug frequency vs frequency of occurrence is shown in Figure 9. This figure shows a dominant frequency of 4.8 slugs per second. The duration of the vapor slugs and the liquid slugs between them was statistically analyzed as shown in Figure 10. The analysis shows the vapor slugs had a duration of about 0.125 second while the liquid slug duration was about 0.08 second. When the slug velocities are determined (future experiments), slug duration and velocity can be used to determine vertical slug size.

Figure 11 shows a plot of dominant vapor slug frequency at 18 inches from the tank bottom, as a function of inlet water temperature (subcooling) for steam flow of 10,000 lbm/hr. and water flow of 3,000 and 5,000 gpm. Also plotted on Figure 11 are frequencies obtained from a second set of experiments (identified as Run No. 2) at the same location and conditions. Reproducibility of the frequency data is good. The frequencies reported in Figure 11 are believed to be the vapor slug formation frequency at their respective flow conditions. This belief was justified through subsequent analysis of other data that showed the same frequency at the 6, 12, and 18-inch level for the same condition.

Rising steam strikes the lower resistivity probe first and then the higher probes. If the time delay between the probe signals indicating steam can be accurately measure, slug velocity can be determined because the probe spacing is known. Present test results (Figure 8 typical) were collected at a slow recorder speed and are not adequate to accurately measure the time delay. Future experiments will be conducted to measure the slug velocity.

The second set of experiments (Run No. 2) was conducted to define the horizontal size of the vapor slug as it moved vertically through the moderator space. Blunt tip (more durable) resistivity probes of the type described in reference 1 were placed at various vertical and radial positions in the tank. Figure 12 shows the vertical placement and Figure 13 shows the radial placement and identification of the probes. Traces from any three resistivity probes could be recorded to determine the average horizontal size of the vapor slug at a particular vertical location. Figure 14 shows a typical record of resistivity signal

vs time at three radial positions at an elevation of 18 inches. The lower slug frequency observed on probe C as compared to A and B, indicates that some slugs were too small to be detected at C. Figures 15, 16, and 17 show maps of percent vapor slugs detected for various operation conditions. The figures show how slug size and vertical penetration change with subcooling and water flow. Note the vertical slug penetration increases as water flow increases and decreases as subcooling increases.

Miniature thermocouple probes in the resistivity probe array (see Figure 5) were used to indicate temperature in and around the voids. A typical trace of resistivity and thermocouple output is shown in Figure 18. The thermocouple response time was observed to be adequate to measure average local slug temperatures at the conditions shown. However, quantitative analysis was not possible because of problems in calibration of the thermocouples.

The results of these tests indicate that for the conditions studied, slug flow is the dominant two-phase flow regime. It is apparent that the steam is contained in large vapor bubbles produced at the bottom of the tank at a frequency determined by the subcooling and steam and water flow rates. The vapor bubbles condense as they move upward through the tank. A theoretical examination of the mechanisms responsible for this condensation is presented in the next section.

### Analytical Model Development

The purpose of the analytical model is to predict the vapor slug size and location within the moderator space at any given time. Such a model can not be fully developed and solved because the necessary experimental data is not available. This section develops the necessary relationships of heat transfer area, bubble velocity, and subcooling to permit formulation of the solution. The model is developed in the following order:

- o Assumptions
- o Heat transfer area:
  - vapor to liquid
  - vapor to tubes
- o Vapor slug velocity
- o Heat transfer mechanisms
  - vapor to liquid (direct)
  - vapor to tube (film)
- o Solution of combined relationship within an energy balance equation.

### Model Assumptions

The analytical model of vapor slug condensation was developed based on the following assumptions:

1. The vapor slug is assumed to be a right circular cylinder of radius  $R$  and height  $x$ , enclosing the lattice tubes.
2. As a consequence of laminar film flow, the liquid film between vapor and tubes is of negligible thickness.
3. Horizontal mixing of the liquid slugs with the outer bulk liquid results in a uniform liquid temperature throughout the tank except in the thin film of liquid between vapor and tubes.
4. The velocity of the steam slug is independent of the curvature of the top surface of the vapor slug, and has only an upward component.
5. The surface temperature of the tubes can be calculated (Appendix A).

### Heat Transfer Area

The size of the steam bubble and the tube geometry has a significant effect on the heat transfer area. Figure 19 shows the assumed geometry of a vapor slug of radius  $R$ , vertical size  $x$  and distance from tank bottom  $y$ , at some time  $t$ . Figure 20 shows the variation of direct vapor-liquid interface perimeter (contact between vapor slug and bulk liquid at bubble circumference) as a function of a slug radius  $R$ . This perimeter is used in equation 10 to calculate vapor slug area in contact with liquid. This curve is piecewise continuous, and was obtained graphically. Figure 21 shows the number and type of tubes in contact with the vapor slug as a function of  $R$ . Two types of tubes are identified, steaming tubes ( $n_s$ ), and water flow tubes, ( $n_w$ ).

### Vapor Slug Velocity Correlation

A relationship must be developed that will predict the slug velocity based on controlling factors. This is necessary to enable prediction of the slug location with time. Because the mass of the vapor slug is small, it will almost instantly reach terminal velocity and therefore the relationship need only apply to the terminal velocity. Two equations to predict bubble velocity were found in the literature<sup>5,6</sup> but neither can be considered directly applicable because of the presence of tubes within the bubble region. Therefore the slug velocity relationship must be experimentally determined and fitted to the

general form:

$$V_b = \frac{dy}{dt} = f(R) + g(m_g, m_f, \Delta T_B) \quad (1)$$

(See Appendix B for nomenclature of this and subsequent equations)

### Heat Transfer Mechanism

Two sources of heat transfer are possibly available to quench the vapor slug. They are direct vapor to bulk liquid condensation and vapor to tube wall (film) condensation, both of which are discussed in Appendix A. The following two sections present the development of the necessary equations for application of the mechanism to the quenching model.

### Direct Vapor-Liquid Condensation

Florschuetz and Chao<sup>7</sup> studied the collapse of stationary spherical vapor bubbles to determine the relative importance of the effects of liquid inertia and heat transfer on the collapse rate. This work resulted in the following criteria for heat transfer dominated collapse:

$$B < .05 \quad (2)$$

where,

$$B = \frac{J_a^2}{\sqrt{C}} \quad (3)$$

$$J_a = \text{Jakob number} = \frac{\rho_f C_p (T_{sv} - T_B)}{\rho_g h_{fg}} \quad (4)$$

$$C = R_o^2 \Delta P / \rho_f K^2 \quad (5)$$

Use of typical test conditions for the present work (Table I) showed the conditions were met and the quenching process is heat transfer controlled.

Wittke and Chao<sup>8</sup> extended the work of Florschuetz and Chao by studying the heat transfer controlled collapse of a spherical bubble under translational motion with respect to the liquid phase. They showed that for high Peclet numbers, the relative velocity of the phases has a significant effect on the condensation rate where;

$$\text{Peclet number} = N_{pe} = \frac{2 V_b(\text{rel}) R_o}{(K/C_p \rho_f)} \quad (6)$$

Estimating a relative velocity of 5 ft/sec for the present work produces a Peclet number of:

$$N_{Pe} = 3 \times 10^6$$

Bankoff and Mason<sup>9</sup> obtained a Nusselt number correlation for heat transfer from a steam bubble to turbulent subcooled liquid. They obtained data for a range of bubble Peclet number of,  $990 \leq N_{Pe} \leq 35,400$ , and developed three correlating equations based on the steam bubble type. The applicable Peclet number is considerably below the present test conditions but it is assumed that the form of the equation is valid:

$$N_{nu} = B'(N_{Pe})^\alpha (N_S)^\beta \quad (7)$$

By the definition of the Nusselt number the heat transfer coefficient is:

$$h_b = (KN_{Nu}) \frac{1}{2R} \quad (8)$$

It is assumed that this heat transfer coefficient is applicable over the entire vapor-liquid interface of the vapor slug and that the temperature of both phases are uniform within the phase. Therefore the heat transferred from the vapor slug directly to the liquid is,

$$Q_b = h_b \dot{V} (\Delta T_B) \quad (9)$$

where,

$$\dot{V} = 2 (\pi R^2 - \pi r^2) [1 + n_s + n_w] + x J(R) \quad (10)$$

### Film Condensation

Filmwise condensation has received a great deal of attention in the literature. For the case of filmwise condensation on the outside surface of a vertical tube, Kreith<sup>10</sup> gives the following correlation for the average heat transfer coefficient assuming laminar film flow and neglecting the effect of vapor shear stress.

$$\bar{h}_i = \frac{4}{3} \left[ \frac{\rho_f (\rho_f - \rho_g) g (h_{fg} + .68 C_p (T_{sv} - T_{si})) K^3}{4 \mu (T_{sv} - T_{si}) x} \right]^{\frac{1}{4}} \quad (11)$$

This form is applicable when,

$$N_{Pr} > 0.5 \quad (12)$$

$$\frac{C_p (T_{sv} - T_{si})}{h_{fg} + .68 C_p (T_{sv} - T_{si})} < 1.0 \quad (13)$$

The criteria for laminar film flow is,

$$\frac{4 \Gamma_c}{\mu_f} < 2000 \quad (14)$$

where,

$$\Gamma_c = \frac{g \rho_f (\rho_f - \rho_g) \delta^3}{3 \mu_f} \quad (15)$$

$$\delta = \left[ \frac{4 \mu_f K x (T_{sv} - T_{si})}{g \rho_f (\rho_f - \rho_g) (h_{fg} + .68 C_p (T_{sv} - T_{si}))} \right] \quad (16)$$

Application of the experimental data to these criteria show that all are applicable and therefore equation 11 can be used.

Because the outside surface temperature of the central (c), steaming (s), and water flow (w) tubes may be different, the total heat transfer rate from the vapor slug to the tubes is

$$\dot{Q}_f = 2\pi r \times \left[ \bar{h}_c \Delta T_c + \eta_s \bar{h}_s \Delta T_s + \eta_w \bar{h}_w \Delta T_w \right] \quad (17)$$

The number of steaming tubes,  $\eta_s$ , and water flow tubes,  $\eta_w$ , are given in Figure 21 as functions of the slug radius, R.

### Conservation of Energy

All of the applicable equations that describe the mechanisms of the quenching process have been developed in the previous sections. It is now necessary to write an energy balance around a control volume, insert the appropriate rate equations and solve. The energy equation is:

$$\dot{m} = \frac{\dot{Q}}{h_{fg}} \quad (18)$$

where,

$$\dot{Q} = \dot{Q}_b + \dot{Q}_f \quad (19)$$

The mass of the vapor slug may be expressed as a function of R and x as,

$$m = \rho_g [\pi R^2 - \pi r^2 (n)] x \quad (20)$$

where:

$$n = 1 + n_s + n_w$$

Differentiating equation (20) with respect to time to produce a rate equation for use in the energy balance produces,

$$\dot{m} = \rho_g [\pi R^2 - \pi r^2 n] \dot{x} + x [2\pi R \dot{R} + \pi r^2 \dot{n}] \quad (21)$$

Equations (9), (17), (18) can now be combined to solve for the heat transfer rate,  $h_b$ ;

$$h_b = \frac{h_{fg} \rho_g (\pi R^2 - \pi r^2 n) \dot{x} + x (2\pi R \dot{R} + 2\pi r^2 \dot{n}) - 2\pi r x (h_c \Delta T_c + n_s h_s \Delta T_s + n_w h_w \Delta T_w)}{2 (\pi R^2 - \pi r^2 n) + x \gamma (R)} \Delta T_B \quad (22)$$

The first term in brackets in the numerator is the heat transfer due to direct vapor-liquid contact and the second term is due to film condensation. By insulating all of the tubes in contact with the vapor slug, film condensation can be prevented and the film contribution may be dropped. Limited experiments have previously indicated that insulation of tubes produces little affect on the total steam volume and therefore film condensation is probably of lesser importance.

Equation (22) may be used with experimental data ( $R, x, \dot{x}, \dot{R}, \Delta T_B, \Delta T_c, \Delta T_s, \Delta T_w$ ) to obtain values of  $h_b$  which may be correlated in terms of a Nusselt number per equation (7). Once a correlation of  $h_b$  is determined and a geometric factor relating x and R is assumed, equation (22) may be integrated to obtain R as a function of time. Substituting the resulting relationship into equation (1) and integrating again yields the vertical position y of the slug at anytime t. Therefore, once the necessary experimental data is obtained and the integrations made, the slug position and size can be fully specified with time.

CONCLUSIONS

Experiments in the RHTF have shown the following for steam injection into subcooled water for the uniform lattice configuration:

- o Slug flow is the dominant two-phase flow regime
- o Vapor slugs form at the bottom of the tank and quench as they rise through the core.
- o The slug formation rate (frequency) is dependent on the steam and water flow rates and the subcooling. The slug formation mechanism is unknown.
- o The condensation process is direct vapor-liquid heat transfer but film condensation on the tubes may also be important.
- o An analytical solution (model) can probably be developed given the following experimental data: Bubble rise and condensation velocity, correlated heat transfer coefficient, bubble frequency and initial bubble size.

REFERENCES

1. Muhlbaier, D. R., "Steam Pocket Formation From A Simulated Nuclear Excursion in a Water-Moderated Reactor Mockup," DP-MS-74-67, (1974).
2. Collier, J. G., "Convection Boiling and Condensation," McGraw-Hill, London, (1972).
3. Muhlbaier, D. R., "Safety Analysis of the Reactor Hydraulic Test Facility, Building 786-A," DPSTSA-700-19, (1973).
4. Muhlbaier, D. R., "Moderator Velocity Study for C&D Conditions," DPST-73-460, (1973).
5. Griffith, P., "The Prediction of Low Quality Boiling Voids," Journal of Heat Transfer, p. 327, (1964).
6. Wallis, G. B., "One-dimensional Two-Phase Flow," McGraw-Hill Book Co., (1969).
7. Florschuetz, L. W., and Chao, B. T., "On the Mechanics of Vapor Bubble Collapse," Journal of Heat Transfer, p. 209, (1965).
8. Wittke, D. D., and Chao, B. T., "Collapse of Vapor Bubbles With Translatory Motion," Journal of Heat Transfer, p. 17, (1967).

REFERENCES, Contd

9. Bankoff, S. G., and Mason, J. P., "Heat Transfer from the Surface of a Steam Bubble in Turbulent Subcooled Liquid Stream," A.I.Ch.E. Journal, p. 30, (1962).
10. Kreith, F., "Principles of Heat Transfer," Second Edition, International Textbook Co., (1969).

DRM:sbc

TABLE 1

TYPICAL EXPERIMENTAL CONDITIONS

$$\dot{m}_g = \text{total steam flowrate} = 1 \times 10^4 \text{ lbm/hr.}$$

$$\dot{m}_l = \text{total water flowrate} = 1.46 \times 10^6 \text{ lbm/hr. (3,000 GPM)}$$

$$T_B = \text{Bulk inlet water temperature} = 79.5^\circ\text{C}$$

$$T_{sv} = \text{saturation temperature in tank} = 106^\circ\text{C}$$

$$\rho_f = \text{density of liquid water} = 60.1 \text{ lbm/ft}^3$$

$$\rho_g = \text{density of saturated vapor @ } T_{sv} = 0.03 \text{ lbm/ft}^3$$

$$C_p = \text{specific heat of liquid water @ film temperature} = 1 \text{ BTU/lbm}^\circ\text{F}$$

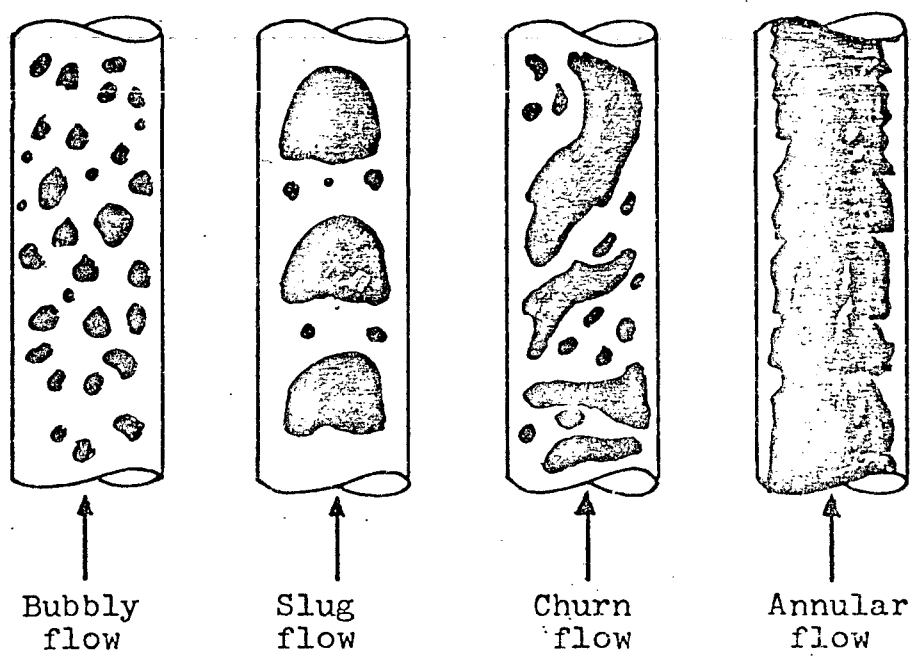
$$h_{fg} = \text{latent heat of condensation} = 970 \text{ BTU/lbm}$$

$$u_f = \text{viscosity of liquid water at film temperature} = 0.74 \frac{\text{lbm}}{\text{ft hr}}$$

$$K = \text{thermal conductivity of liquid water at film temperature} \\ = 0.394 \frac{\text{BTU}}{\text{hr ft}^\circ\text{F}}$$

$$T_{\text{film}} = \text{film temperature} = \frac{T_{sv} + T_B}{2} \approx 93^\circ\text{C}$$

$$\sigma = \text{liquid-vapor interface surface tension} = 0.004 \frac{\text{lb}_f}{\text{ft}}$$



REGIMES OF TWO PHASE  
VERTICAL FLOW  
FIG. 1

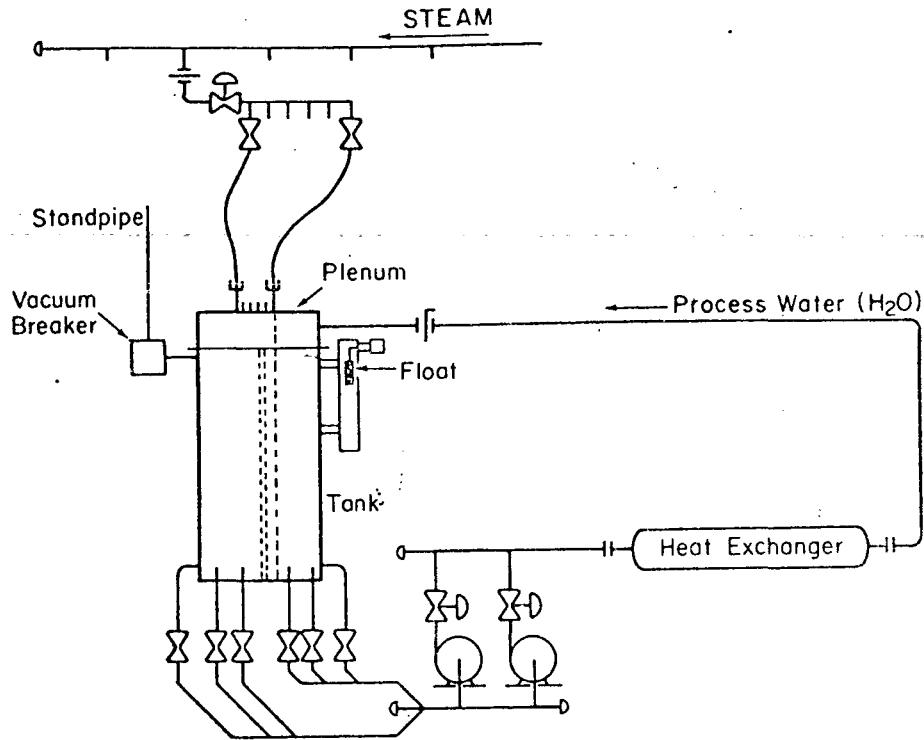
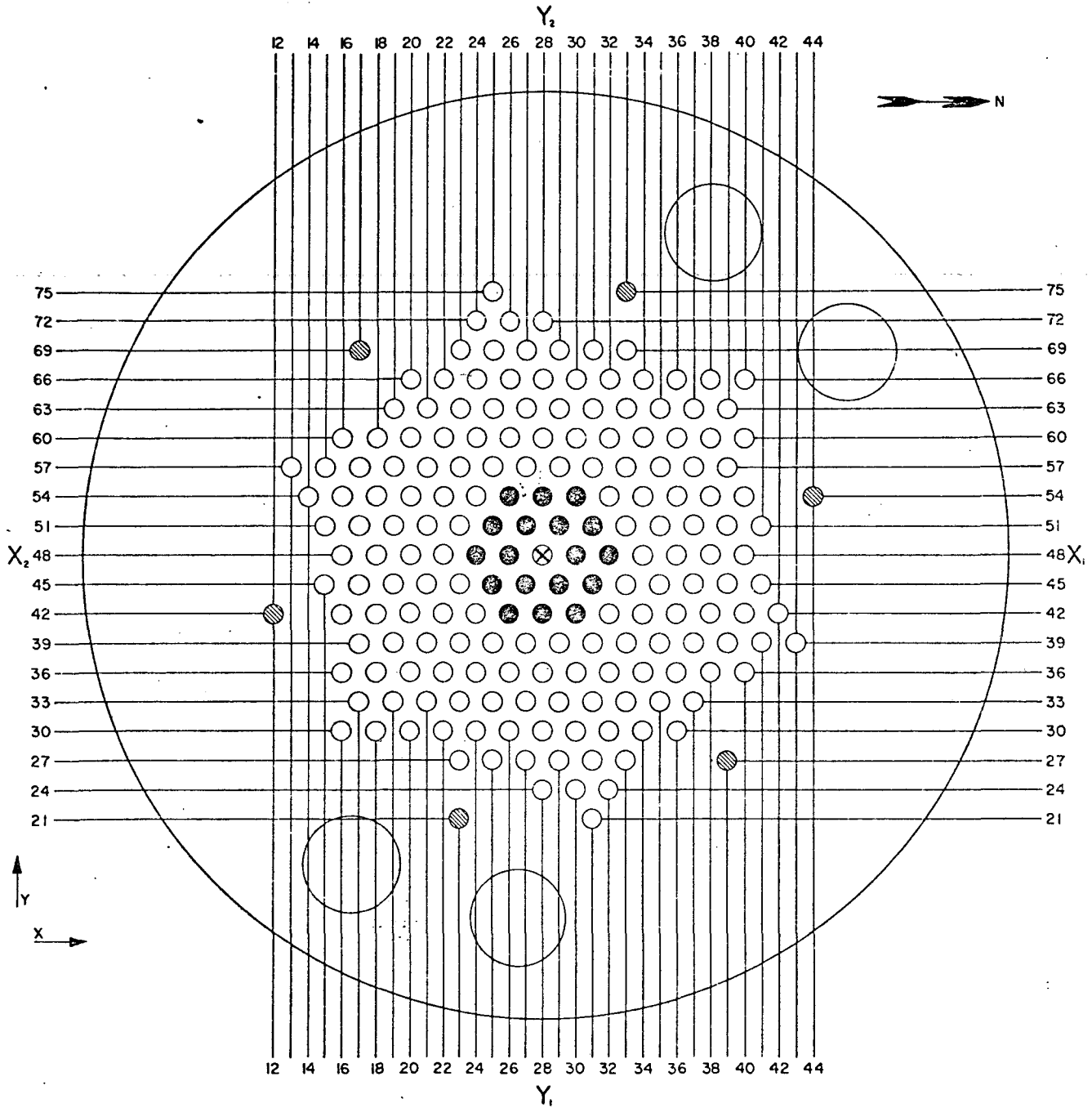
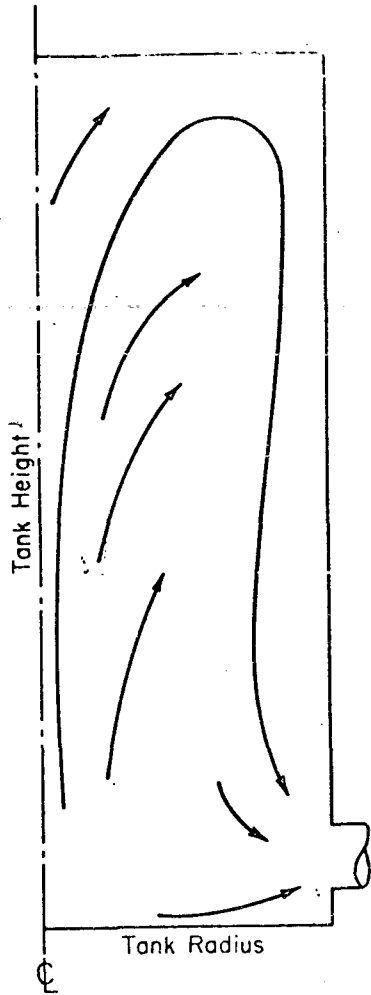


FIG. 2. Reactor Hydraulic Test Facility



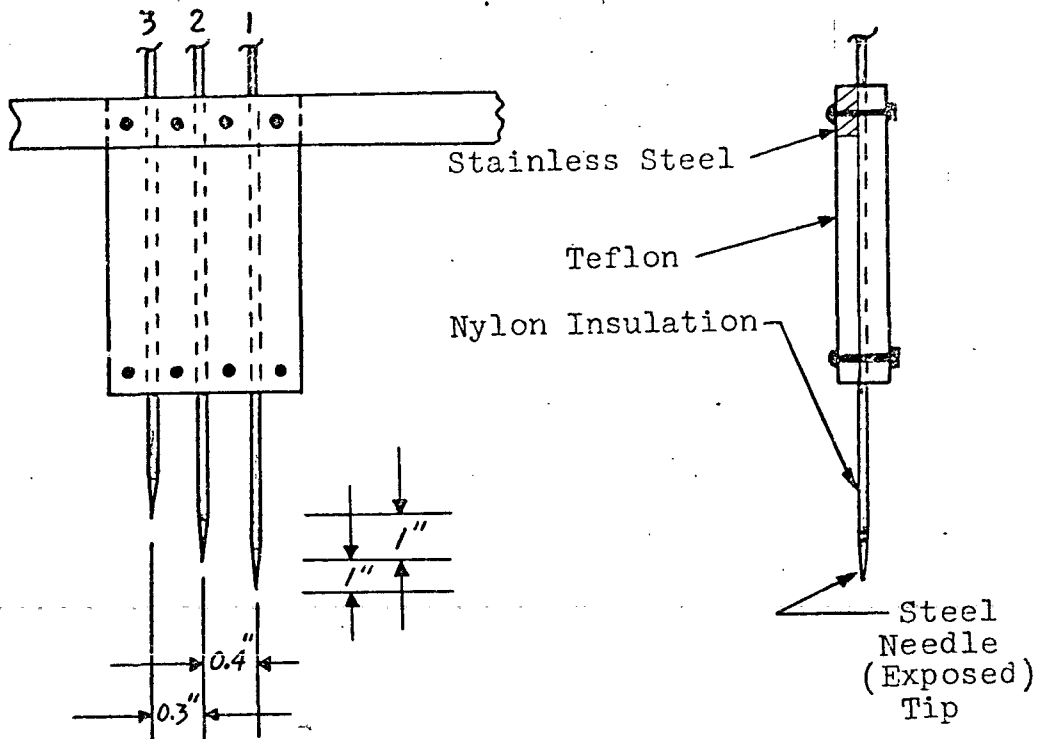
- Steam Injected
- ⊗ No Flow
- Water Injected
- ▨ Support Rods

Assembly Tube Positions for a Uniform Lattice  
FIG. 3



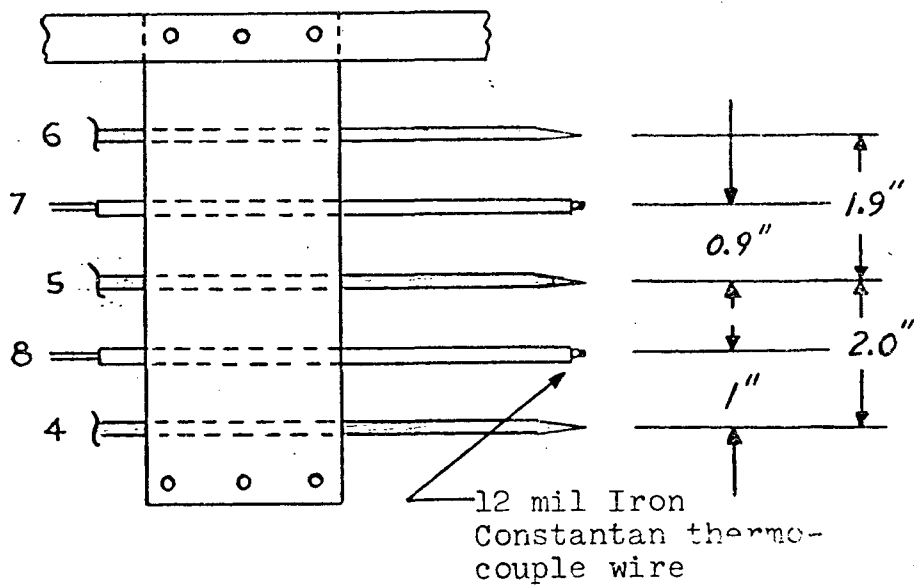
Bulk Moderator Flow Pattern in the  
Reactor Hydraulic Test Facility (No Steam)

FIGURE 4



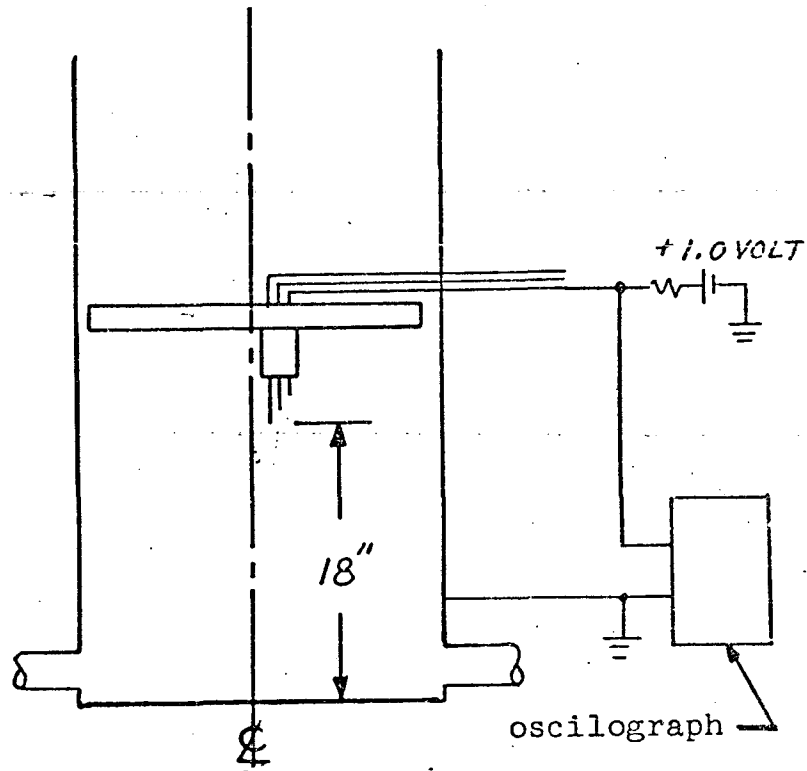
VERTICAL TYPE RESISTIVITY PROBES

FIGURE 5



HORIZONTAL TYPE  
RESISTIVITY & TEMPERATURE PROBE

FIG. 6



PLACEMENT OF VERTICAL PROBE IN TANK, RUN #1

FIG. 7

TYPICAL VERTICAL RESISTIVITY PROBE DATA

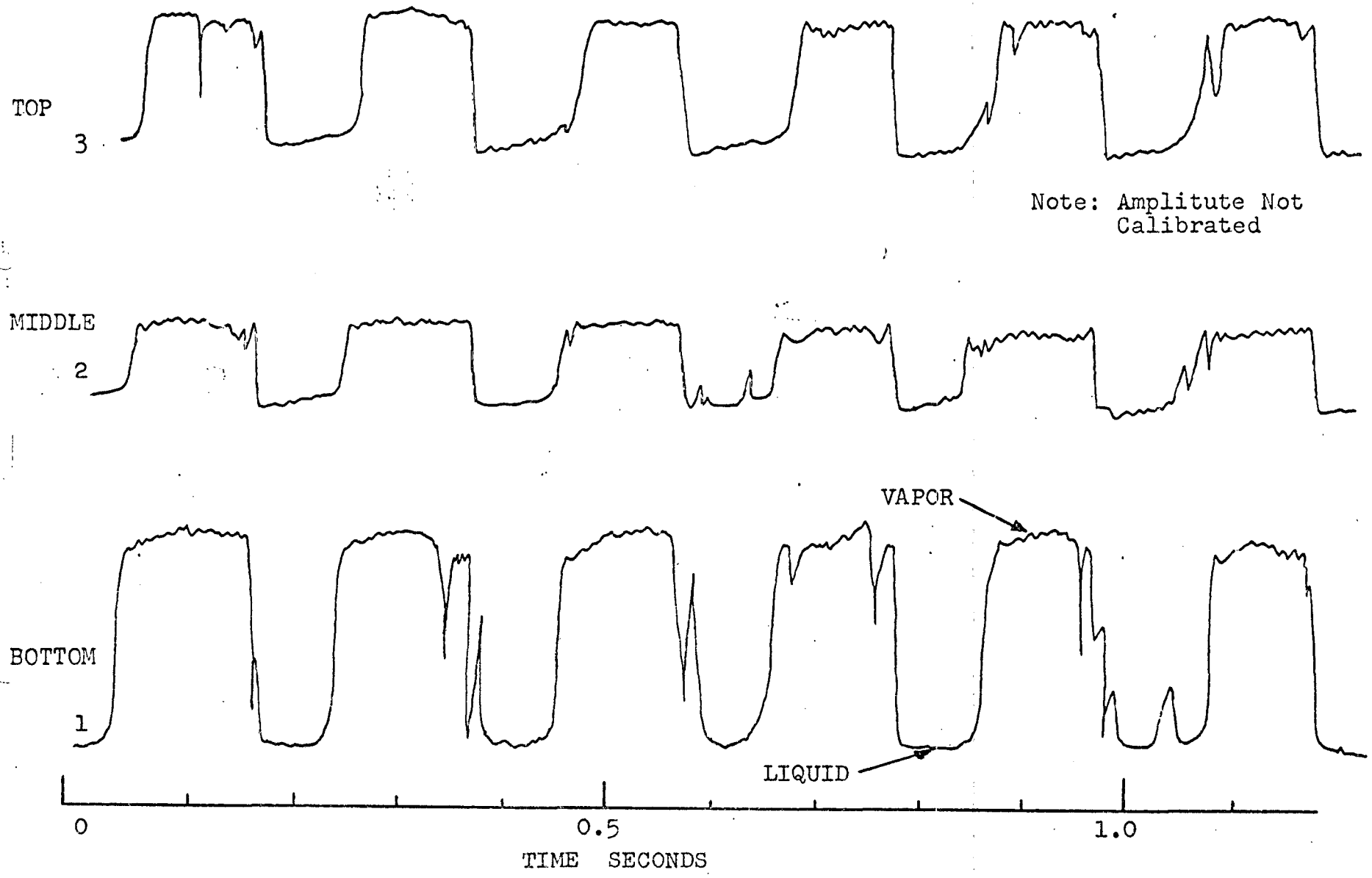
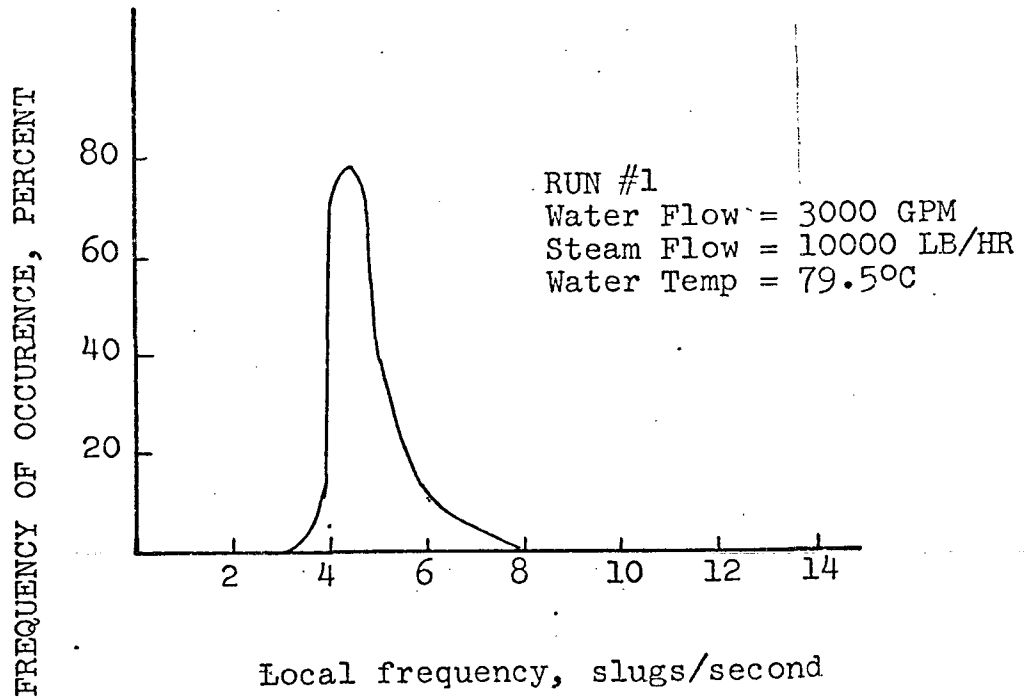
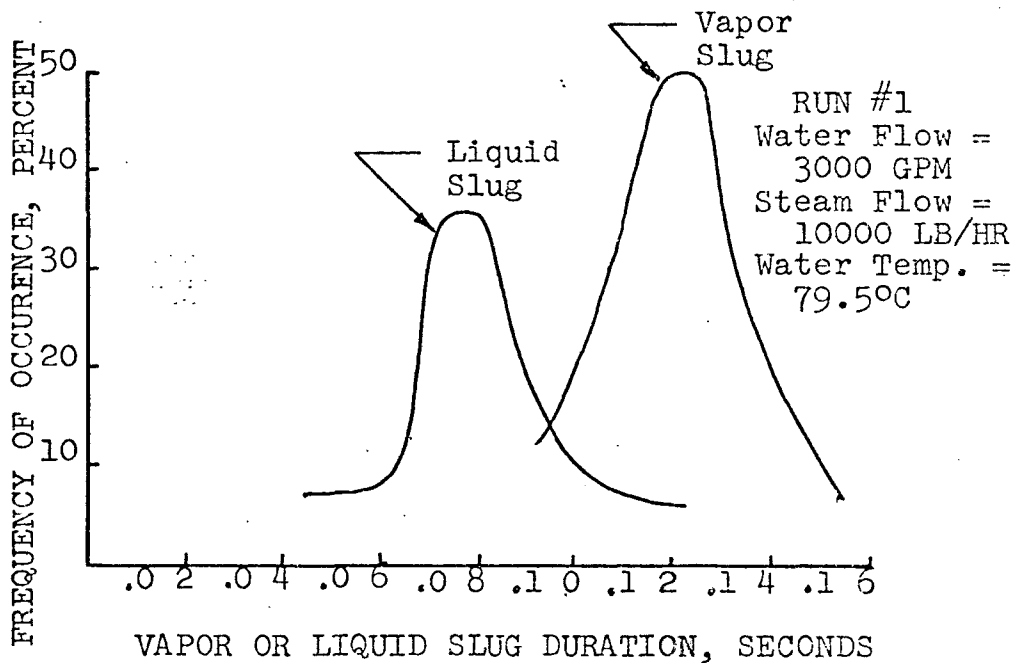


FIG. 8



NORMALIZED SLUG FREQUENCY

FIG. 9



NORMALIZED SLUG DURATION

FIG. 10

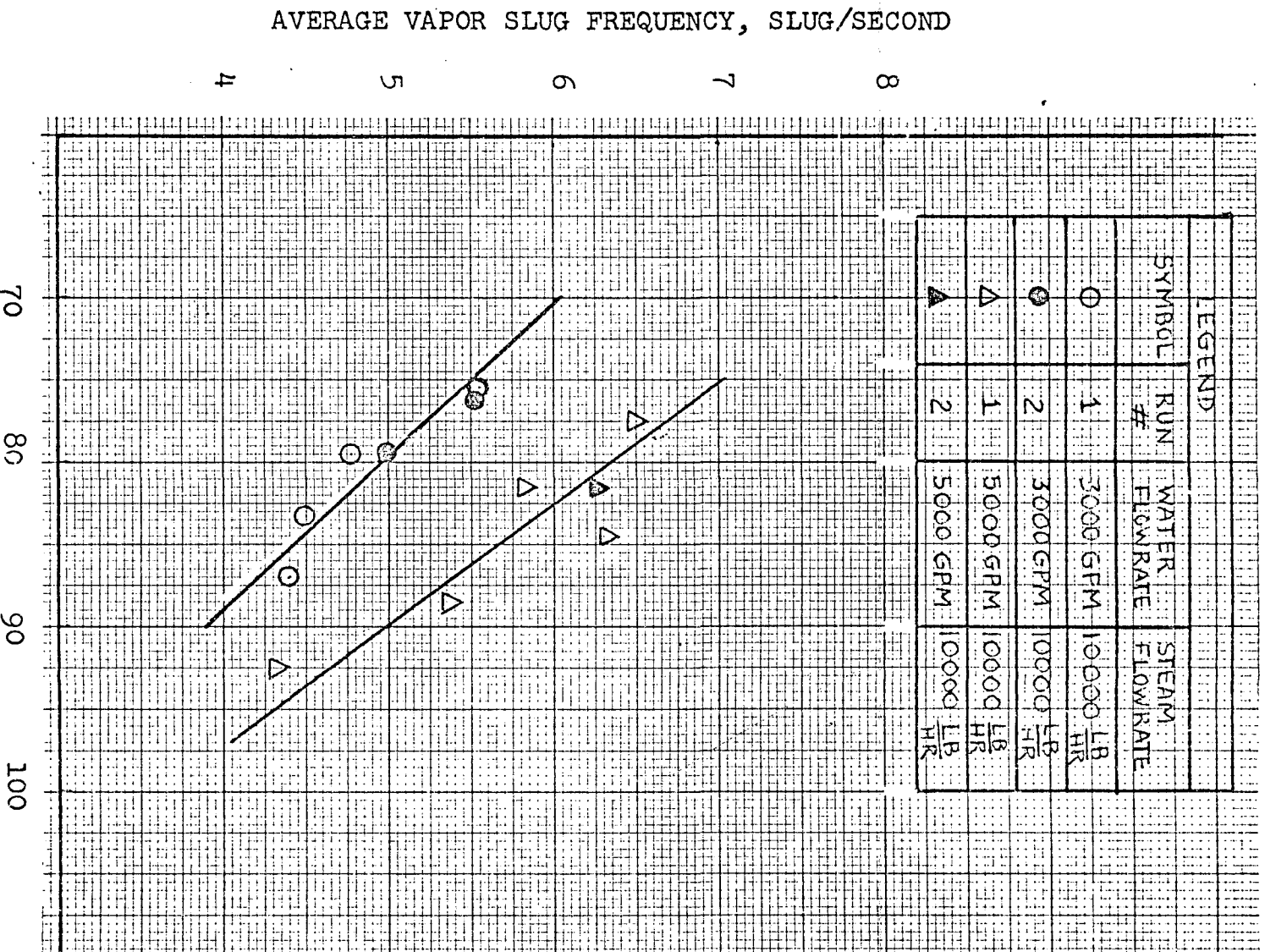
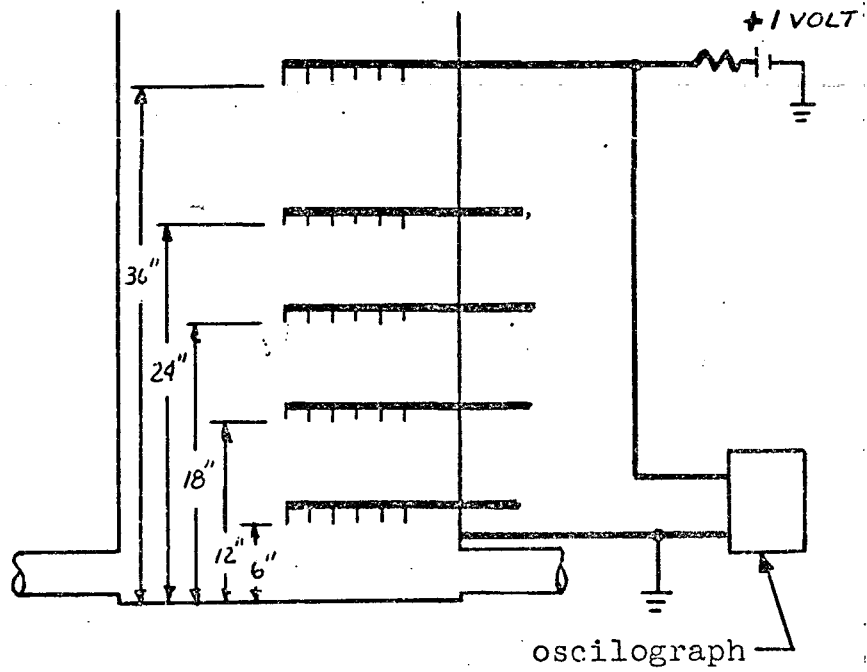
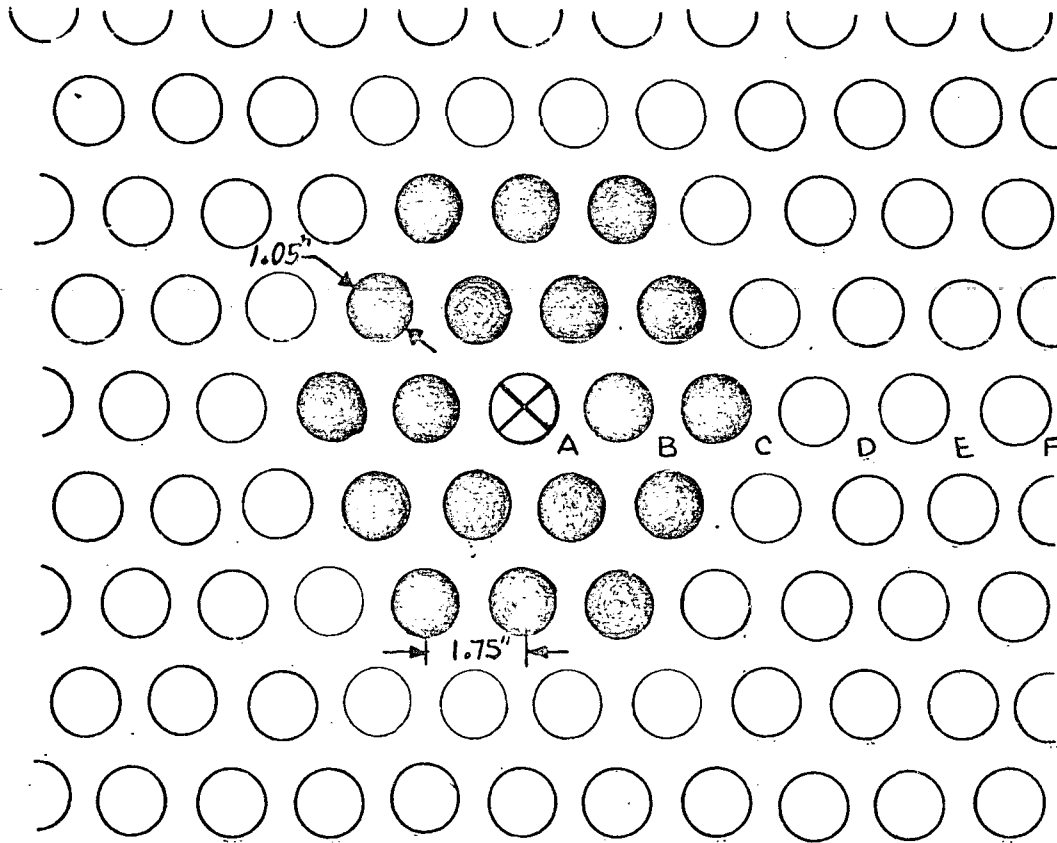


FIG. 11 AVERAGE VAPOR SLUG FREQUENCY  
(18" FROM TANK BOTTOM)



PLACEMENT OF RESISTIVITY  
PROBES FOR RUN #2

FIGURE 12



- - Water Tubes
- - Steam Tubes
- A to F - Resistivity Probes

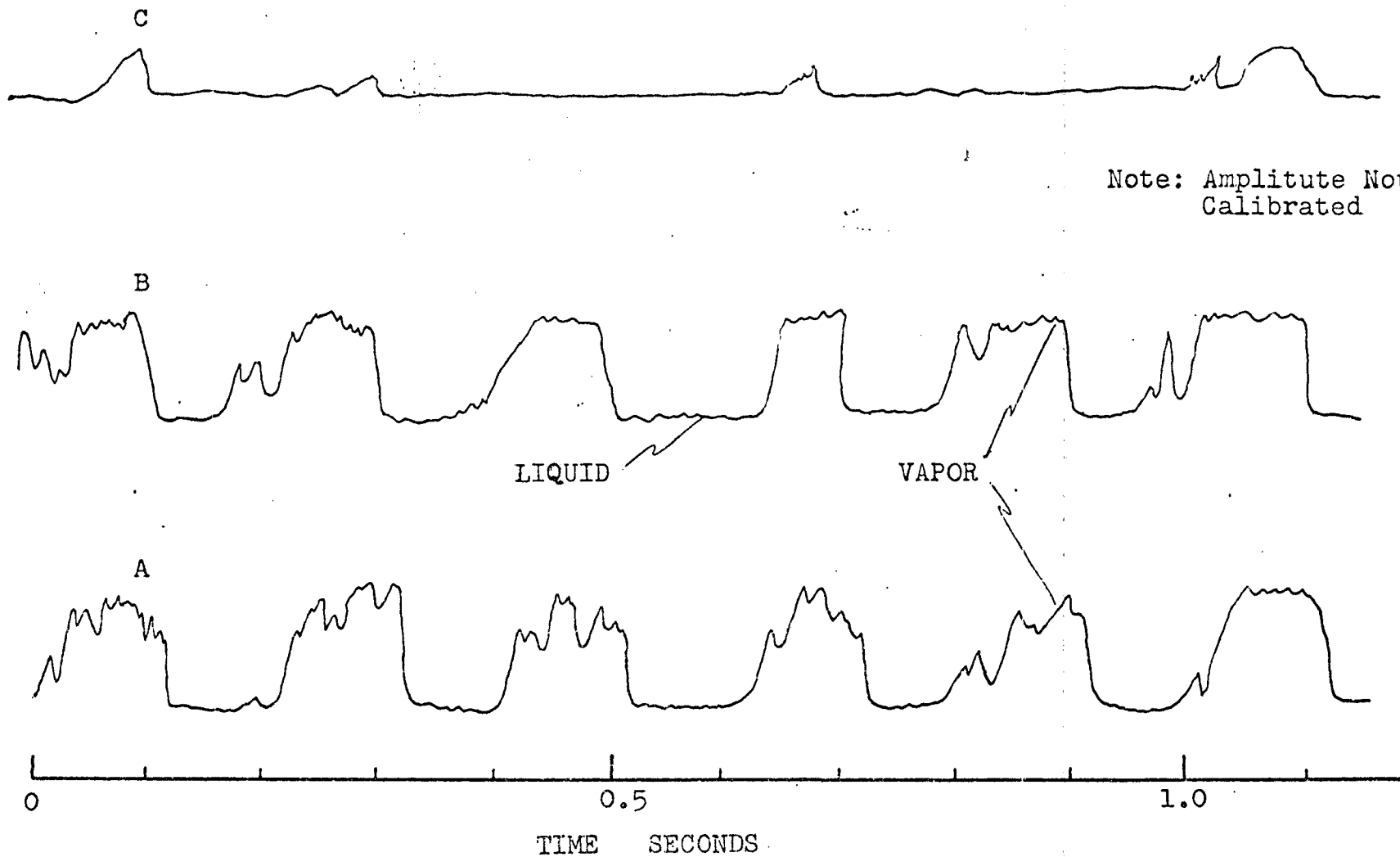
RADIAL PLACEMENT OF RESISTIVITY PROBES

FIGURE 13

TYPICAL RESISTIVITY PROBE SIGNALS

RUN # 2 DISTANCE ABOVE TANK BOTTOM = 18 INCHES  
STEAM FLOW = 10,000 LB/HR WATER FLOW = 3000 GPM @ 79.5 °C

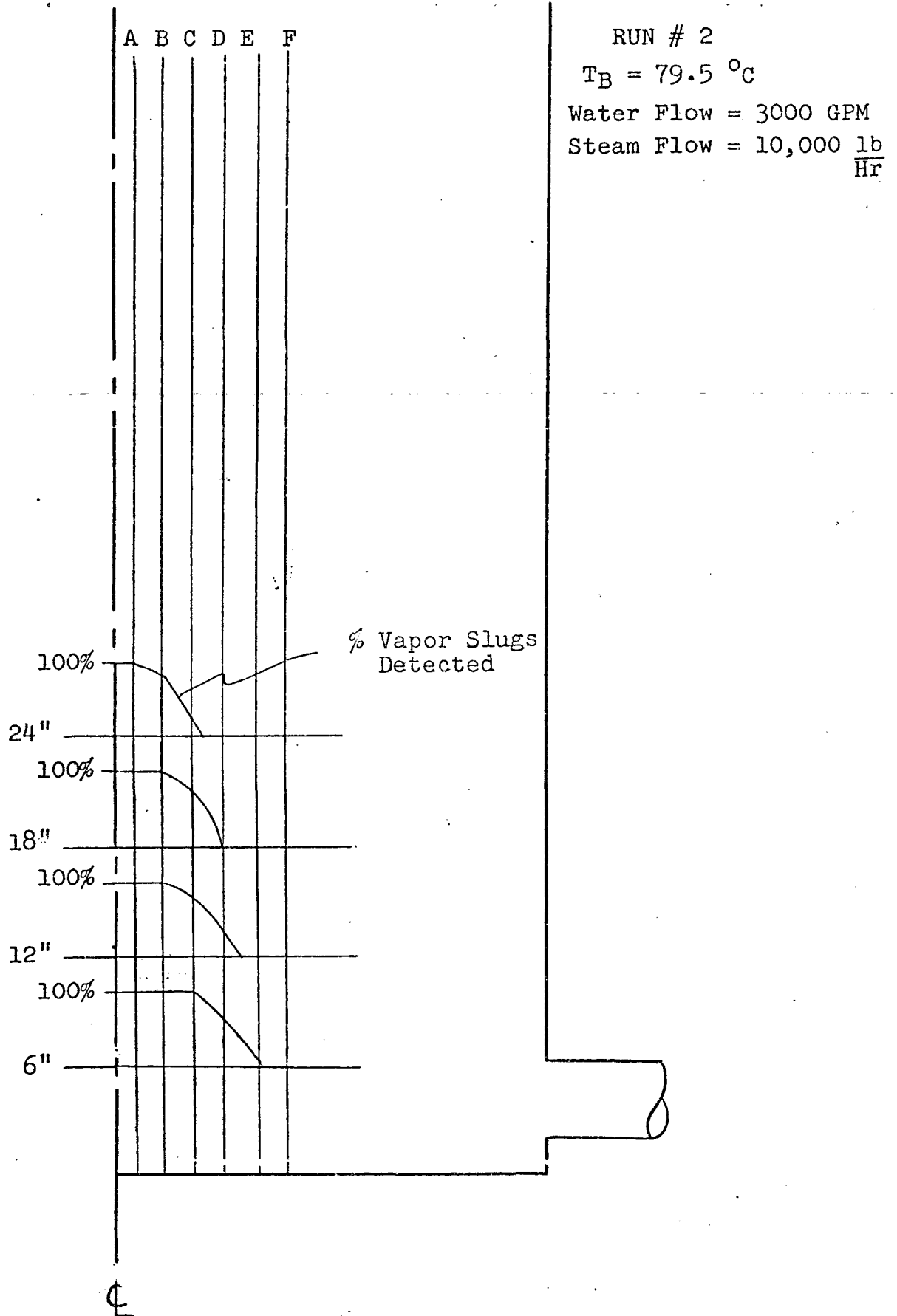
G. F. MERZ



-24-

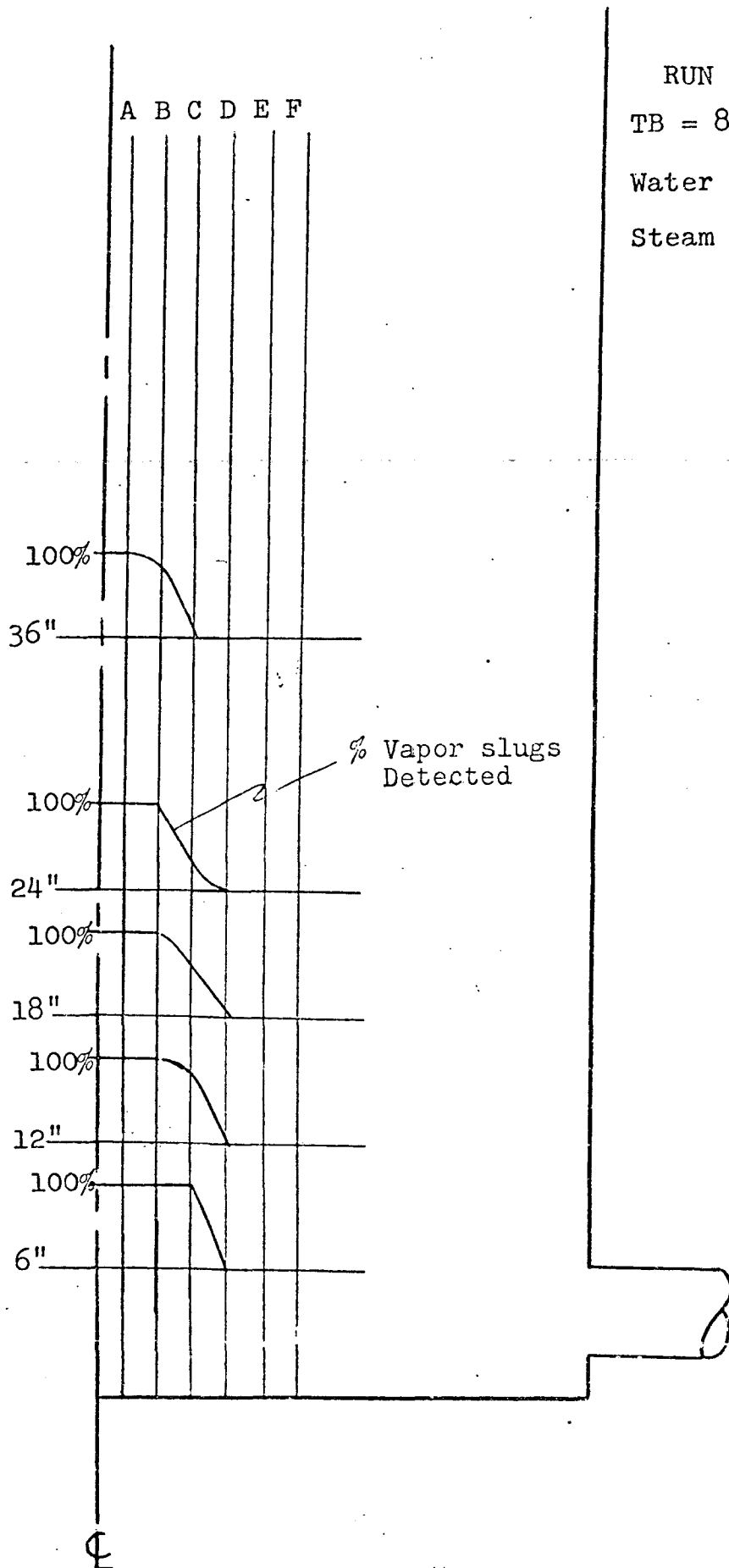
DPST-76-242

FIG. 14



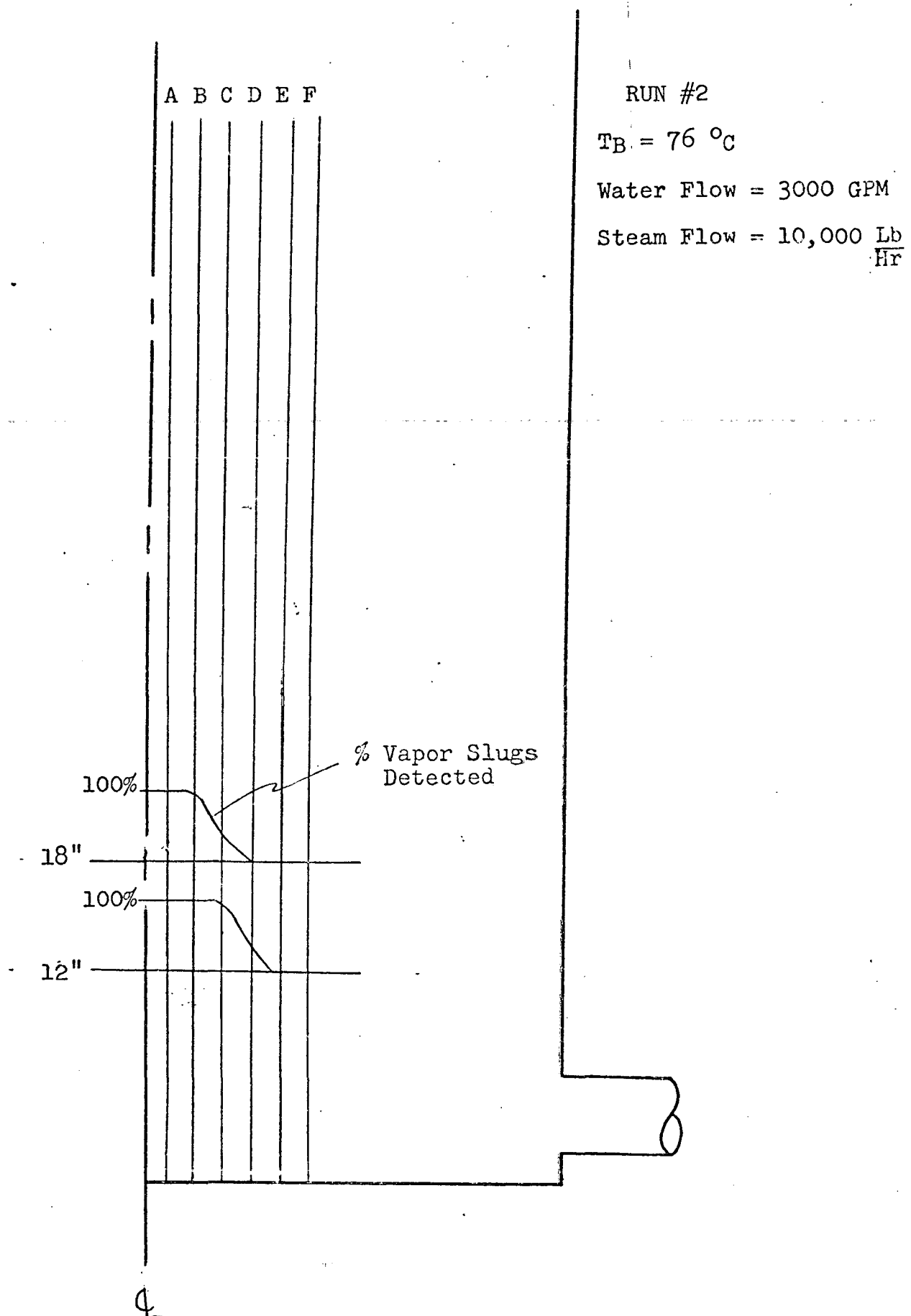
VAPOR SLUG HORIZONTAL MAPPING

FIG. 15



RUN # 2  
TB = 81.5 °C  
Water Flow = 5000 GPM  
Steam Flow = 10,000  $\frac{\text{Lb}}{\text{Hr}}$

VAPOR SLUG HORIZONTAL MAPPING  
FIG. 16



RUN #2

T<sub>B</sub> = 76 °C

Water Flow = 3000 GPM

Steam Flow = 10,000  $\frac{\text{Lb}}{\text{Hr}}$

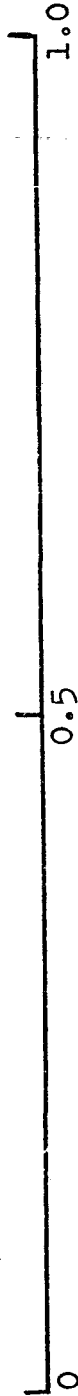
VAPOR SLUG HORIZONTAL MAPPING

FIG. 17

TYPICAL HORIZONTAL RESISTIVITY & TEMPERATURE  
PROBE DATA RUN # 2

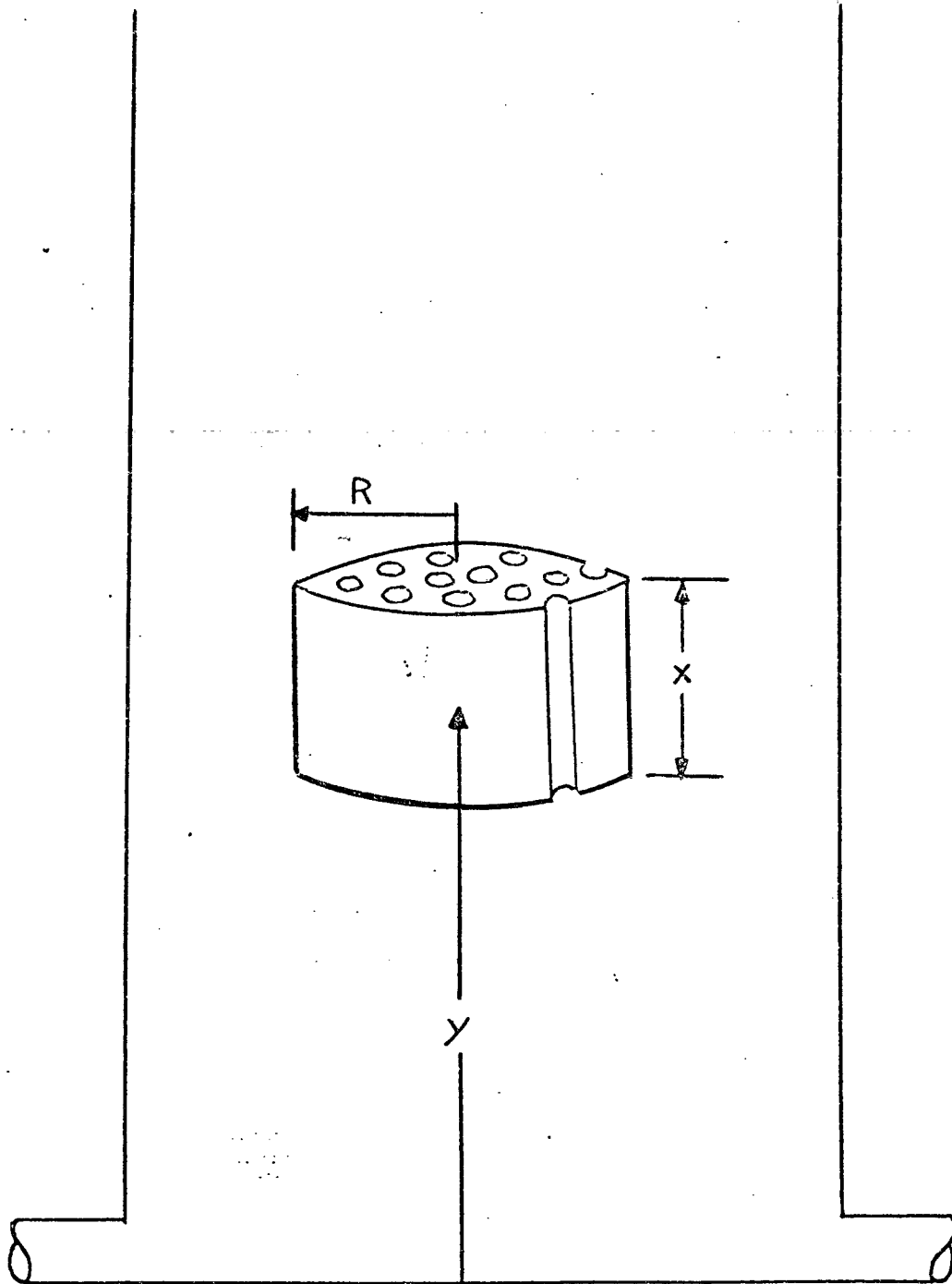


Note: Amplitude Not  
Calibrated



TIME, SECONDS

FIG. 18



ASSUMED VAPOR SLUG GEOMETRY

FIG. 19

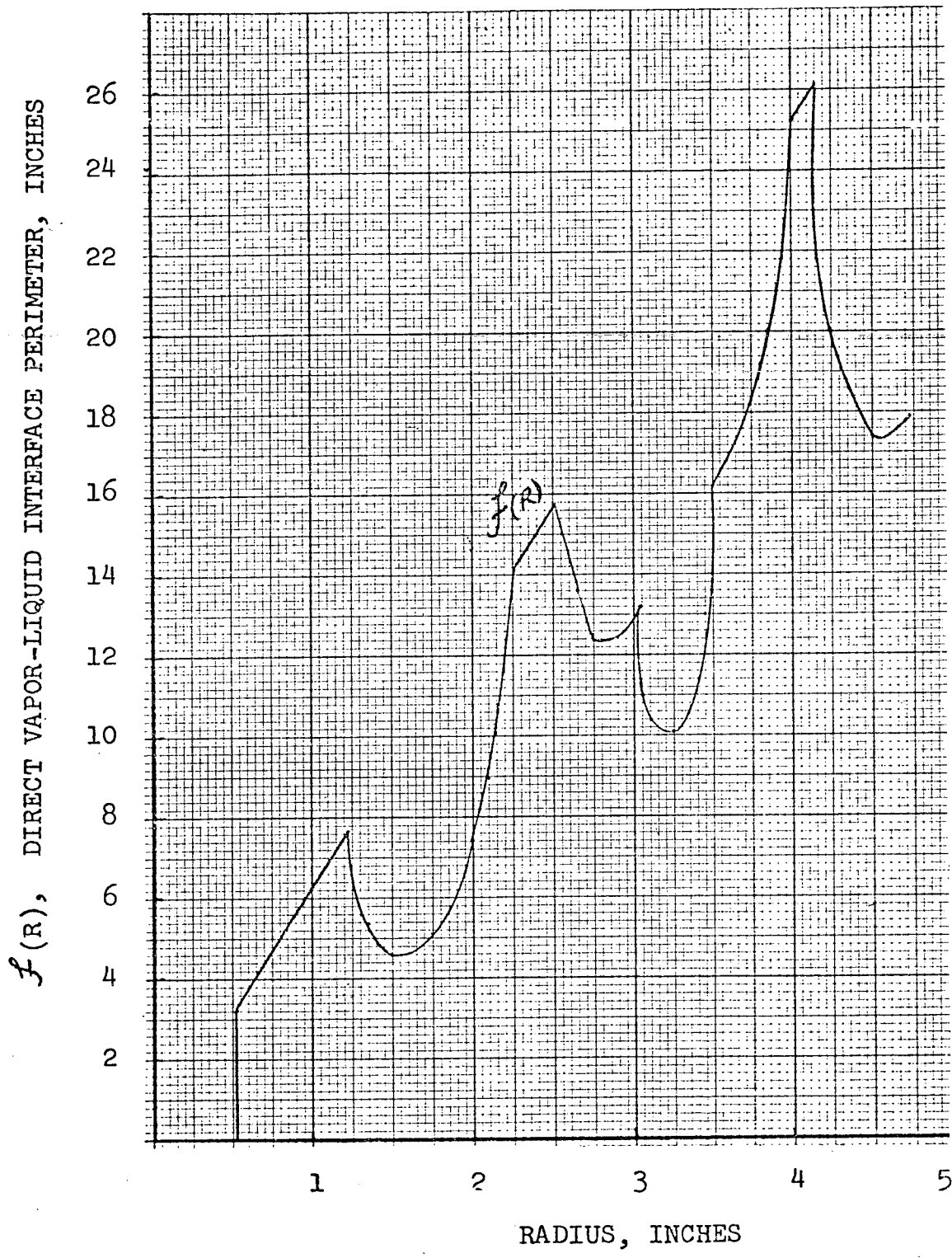


FIG. 20 DIRECT VAPOR-LIQUID INTERFACE PERIMETER

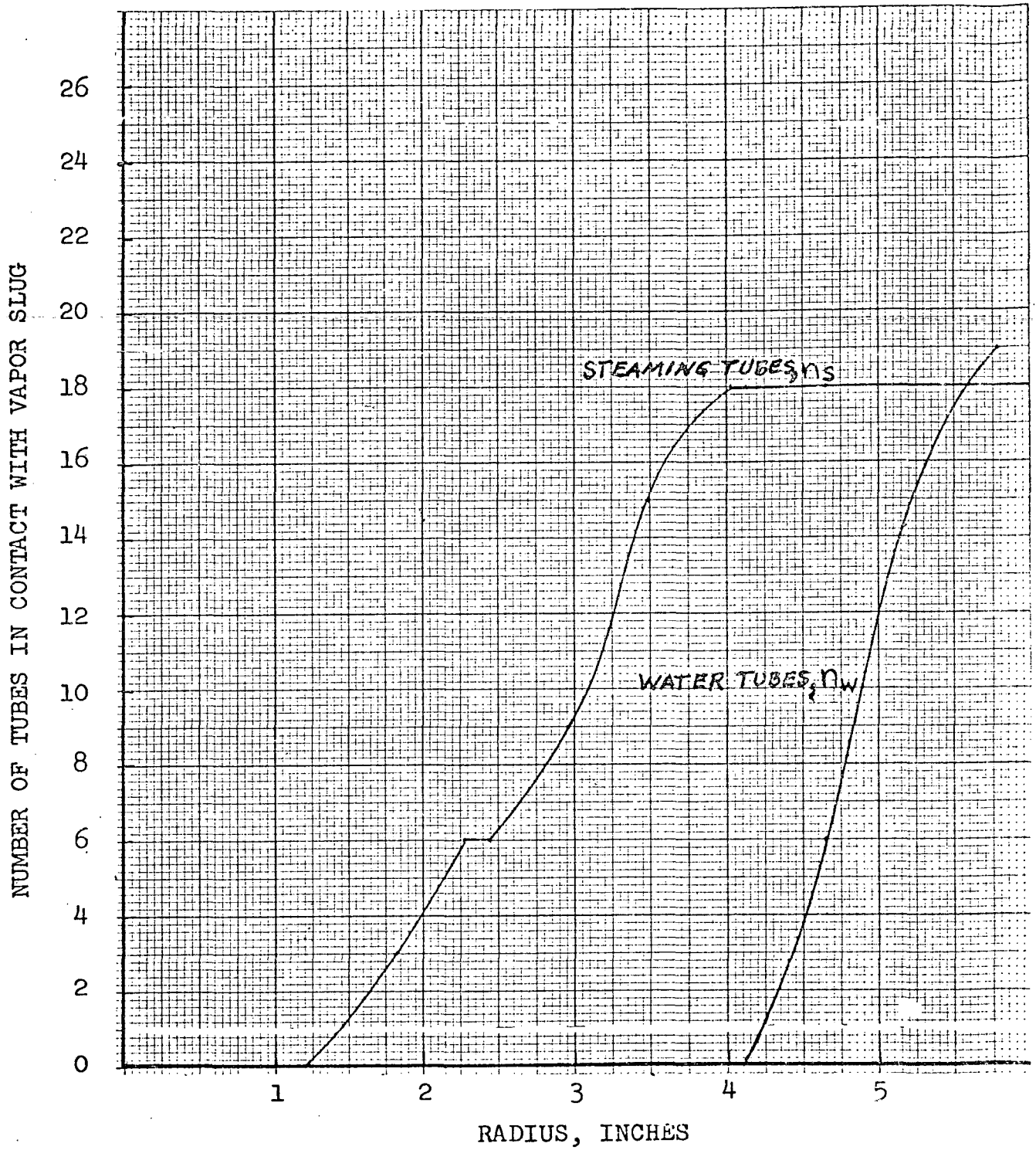


FIG. 21 NUMBER OF TUBES IN CONTACT WITH VAPOR SLUG (UNIFORM LATTICE CASE)

APPENDIX ACalculated Steam Quenching Mechanisms

Both film condensation on the tube walls and direct vapor-liquid condensation may be an important mechanism of vapor slug quenching. Both processes have been included in the model. This appendix examines the relative importance of the two mechanisms for a typical case (see data, Table I).

The outside tube wall temperature must be known to determine the rate of vapor quenching. Because this temperature can not be easily measured accurately, it has been calculated by determining the tube internal temperature (based on steam pressure) and the temperature drop across the tube wall. The pressure within the tube is defined by the following equation for the conditions shown in Figure A1;

$$P - P_{\text{bulk}} = 6.56 \times 10^{-5} \left( \frac{\dot{m}g}{n_{\text{stot}}} \right)^2 \quad (\text{A1})$$

For  $P_{\text{bulk}} = 19$  psia

$$P \approx 39.2 \text{ psia}$$

The following assumptions have been made so that the surface temperature could be estimated (see Figure A2),

- o No axial variation in temperature,  $T_{\text{wi}}$ , or pressure  $P$ , of the steam inside the tube
- o The passage of steam slugs external to the tube has negligible effect on the outside wall temperature,  $T_{\text{wo}}$ .
- o Steam inside of the tube is near saturated vapor, i.e., high quality.

At a pressure of 39.2 psia the saturation temperature is,

$$T_{\text{sat}} = 266^{\circ}\text{F}$$

while the bulk temperature is,

$$T_{\text{B}} = 176^{\circ}\text{F}$$

The Reynolds number inside the tube is defined as,

$$N_{\text{Re}} = (\text{ID}) \frac{V}{\mu} \quad (\text{A2})$$

from continuity,

$$V_p = \frac{4}{\pi} \frac{\dot{m}_g}{n_{stot}} \frac{1}{\mu(ID)^2} \quad (A3)$$

Therefore,

$$N_{Re} = \left( \frac{4}{\pi} \right) \left( \frac{\dot{m}_g}{n_{stot}} \right) \left( \frac{1}{\mu(ID)} \right) \quad (A4)$$

For the case of interest (Table I)

$$N_{Re} \cong 3 \times 10^5 \quad (\text{Turbulent flow})$$

Since the turbulence is high inside the tube, the following simplification is justified.

$$T_{wi} \cong T_{sat} \quad (A5)$$

The problem is now to find the outside wall temperature of the tube. An energy balance per unit area at the outside surface of the tube can be written,

$$h_o (T_{wo} - T_B) = \frac{K_{ss}}{w} (T_{sat} - T_{wo}) \quad (A6)$$

where,

$$\begin{aligned} K_{ss} &= \text{thermal conductivity of 304 stainless steel} \\ &= 9.4 \text{ BTU/hr ft}^\circ\text{F} \end{aligned}$$

$$w = \text{tube wall thickness} = 0.0094 \text{ ft}$$

Previous estimates of  $h_o$ , which are consistent with the film heat transfer values derived in this appendix, are of the order of,

$$h_o \cong 1500 \text{ BTU/hr ft}^2\text{F}$$

Solving equation (A6) for  $t_{wo}$

$$T_{wo} = \left( \frac{1}{h_o + \frac{K_{ss}}{w}} \right) \left[ \frac{K_{ss}}{w} T_{sat} + h_o T_B \right] \quad (A7)$$

substituting,

$$T_{wo} = 211.9^\circ\text{F} \quad (\text{or approximately } 100^\circ\text{C})$$

Therefore all steaming tubes have been assumed to have an outside temperature of,

$$T_{ss} = 100^\circ\text{C}$$

An estimate of the surface temperature of the central (no flow) tube and the water tubes is also required. Since the central tube was partially filled with water and closed off, it will be assumed that its surface temperature is,

$$T_{sc} \approx \frac{T_{sv} - T_B}{2} \approx 93^\circ\text{C}$$

Also, since the water flow tubes are mostly surrounded by the bulk liquid, assume,

$$T_{sw} \approx T_B = 80^\circ\text{C}$$

Applying equation (7)(11) with the above surface temperatures and the data of Table I,

$$h_c = 1514 \text{ BTU/hr}^\circ\text{F ft}^2$$

$$h_s = 1833 \text{ BTU/hr}^\circ\text{F ft}^2$$

$$h_w = 1278 \text{ BTU/hr}^\circ\text{F ft}^2$$

From equation (11) and (17),

$$\dot{Q}_f = 2 \text{ rx}^{3/4} [C_c \Delta T_c + n_s C_s \Delta T_s + n_w C_w \Delta T_w] \quad (\text{A8})$$

From equation (8), (9) and (10),

$$\dot{Q}_b = \frac{K}{2R} (N_{Nu}) \quad 2 [\pi R^2 - \pi r^2 (1 + n_s + n_w)] + x \pi (R) \Delta T_B \quad (\text{A9})$$

Now calculate  $\dot{Q}_b$  and  $\dot{Q}_f$  at the following conditions to determine their relative importance,

$$R = 0.354 \text{ ft (4.25 inches)}$$

$$x = 1.0 \text{ ft}$$

From Figure 20

$$(R = 4.25 \text{ inches}) = 1.67 \text{ ft}$$

From Figure 21,

$$n_s = 18, n_w = 1.5$$

Extending Bankoff and Mason's<sup>6</sup> correlation to a Peclet number of  $3 \times 10^6$ , assuming unit Strouhal number, the estimate of the Nusselt number for both the smooth and irregular bubble case is,

$$N_{Nu} \text{ smooth} = 7 \times 10^7$$

$$N_{Nu} \text{ irregular} = 9 \times 10^3$$

Certainly if the smooth bubble correlation were employed,  $\dot{Q}_b \approx \dot{Q}$ . However, there is no reason to assume the smooth over the irregular bubble correlation. Therefore, to show a conservative calculation, the irregular correlation is used so that,

$$N_{Nu} \approx 9 \times 10^3$$

Calculating  $\dot{Q}_f$  and  $\dot{Q}_b$ ,

$$\dot{Q}_f \approx 1 \times 10^5 \text{ BTU/hr}$$

$$\dot{Q}_b \approx 5 \times 10^5 \text{ BTU/hr}$$

Since these numbers are of the same order of magnitude, film condensation must be considered at this stage of the work. By correlation of data for  $N_{Nu}$  (for insulated tubes) the results may show that film condensation is small, however, this has yet to be conclusively demonstrated.

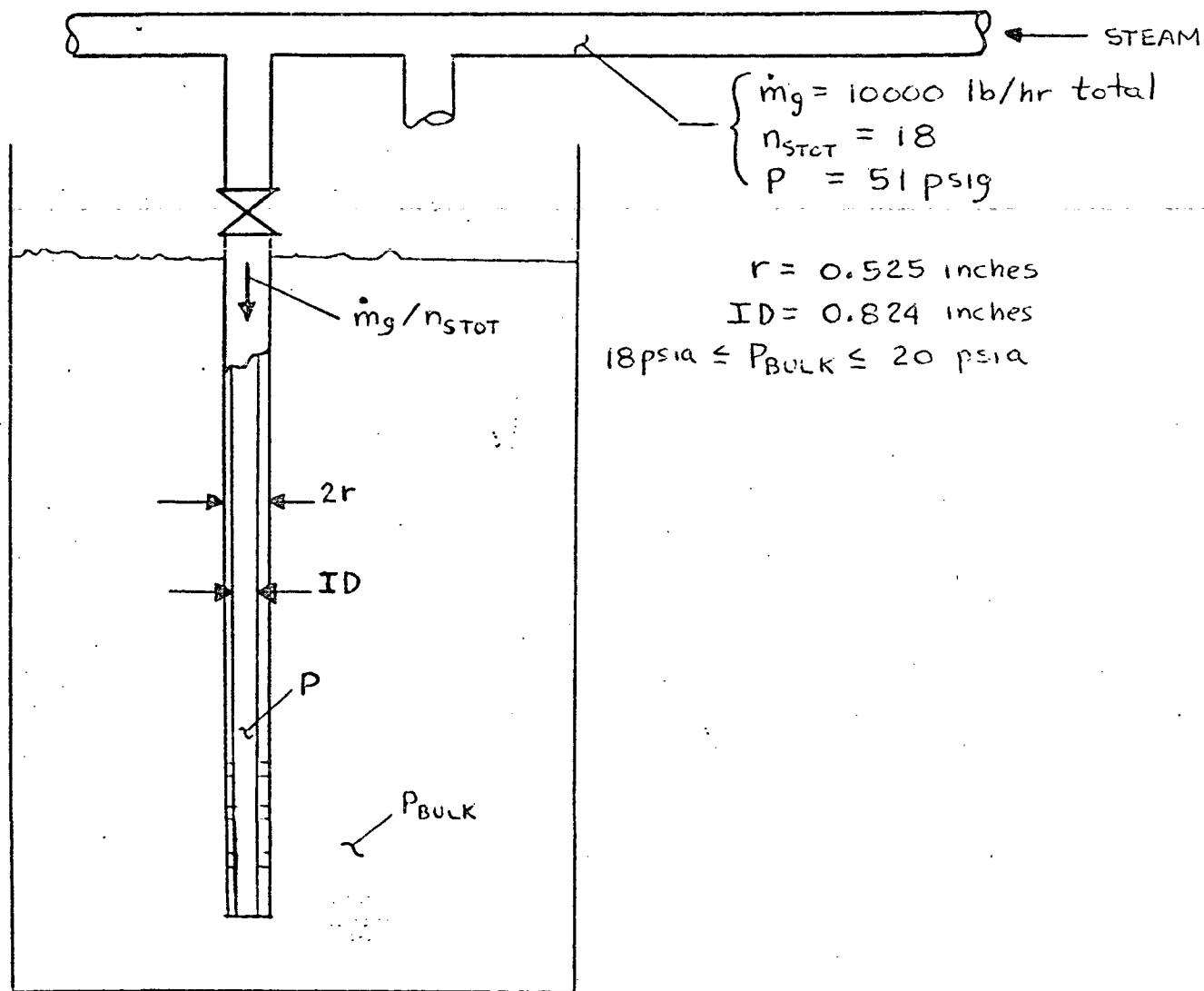
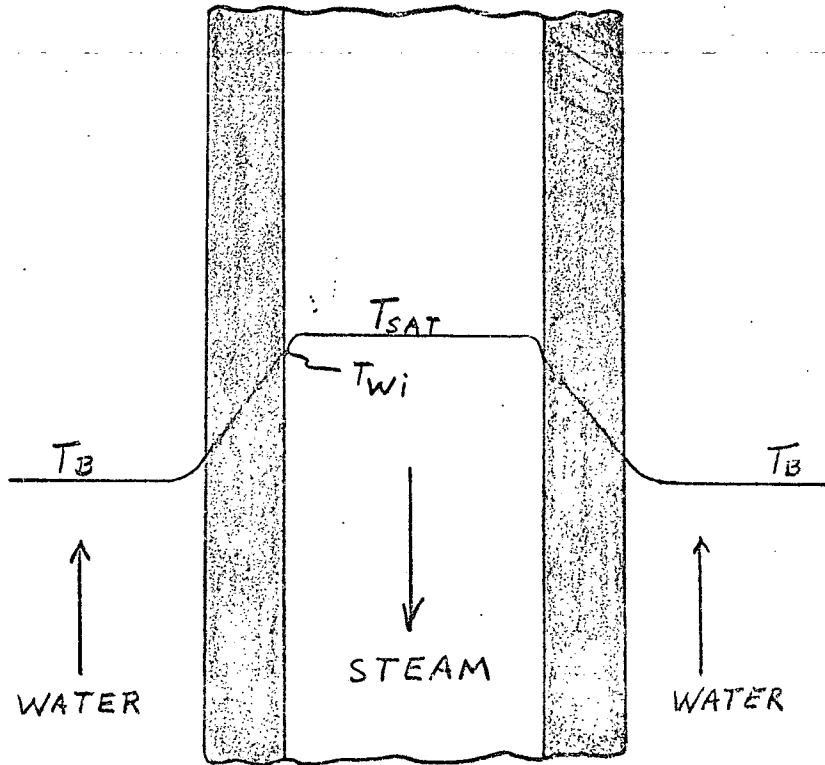


FIG. A1

SKETCH OF TYPICAL TUBE USED IN  
UNIFORM LATTICE GEOMETRY



SECTION OF STEAMING TUBE

FIGURE A2

APPENDIX B  
NONMENCLATURE

- total vapor-liquid surface area defined by equation (10).
- A shroud cross-sectional area.
- B nondimensional number defined by equation (3).
- B' constant defined by equation (7).
- $C_p$  specific heat of liquid water at film temperature.
- (R) vapor-liquid contact perimeter (direct contact between vapor and bulk liquid on slug circumference), see figure 20.
- g gravitational constant.
- $h_b$  heat transfer coefficient for direct vapor-liquid condensation heat transfer.
- $h_{fg}$  latent heat of condensation at saturation temperature,  $T_{sv}$ .
- $h_i$  heat transfer coefficient for filmwise heat transfer to tubes  $i = c, s, w$ .
- $h_o$  average outside convective heat transfer coefficient for external liquid flow, see equation (A6).
- ID inside diameter of tube  $i = c, s, w$ .
- Ja Jakob number defined by equation (4).
- K thermal conductivity of liquid water at film temperature.
- $K_{ss}$  thermal conductivity of 304 stainless steel.
- m mass of vapor slug.
- $\dot{m}$  vapor slug mass condensation rate.
- $\dot{m}_g$  total mass flowrate of steam through tubes.
- $\dot{m}_f$  total mass flowrate of bulk water through tubes.
- $N_{Nu}$  Nusselt number,  $2 Rh_b/K$
- $N_{pe}$  Peclet number,  $2 V_{b(rel)} R_o / (K/cp_f)$

- $N_{Pr}$  Prandtl number,  $C_p \mu / K$
- $N_{Re}$  Reynolds number (ID)  $\frac{V}{\mu}$
- $N_s$  Strouhal number  $V_b / (V_b - V_b(\text{rel}))$
- $n$   $n = 1 + n_s + n_w$ .
- $\dot{n}$  rate of change of  $n$  with time.
- $n_i$  number of tubes of type  $i = s, w$  that are in contact with a vapor slug of radius  $R$ , see Figure 21.
- $n_{stot}$  total number of steaming tubes.
- $P$  pressure in steam tubes in psia.
- $P_{bulk}$  pressure of bulk liquid at tank bottom in psia.
- $Q_f$  total volumetric flow rate of liquid water into tank.
- $\dot{Q}_g$  total volumetric flow rate of steam into tank.
- $\dot{Q}$  vapor slug heat transfer.
- $\dot{Q}_f$  vapor slug heat transfer due to filmwise heat transfer.
- $\dot{Q}_b$  vapor slug heat transfer due to direct vapor - liquid heat transfer.
- $R$  radius of vapor slug.
- $\dot{R}$  rate of change of vapor slug radius.
- $r$  outside radius of tubes.
- $R_0$  initial radius of spherical bubble.
- $T_{sat}$  Saturation temperature inside steaming tubes @ pressure  $P$ .
- $T_{si}$  surface temperature of tube  $i = c, s, w$ .
- $T_{wi}$  steaming tube inner surface temperature.
- $T_{wo}$  steaming tube outer surface temperature,  $T_{ss} = T_{wo}$ .
- $T_{sv}$  saturation temperature at tank bottom.
- $T_B$  bulk liquid water inlet temperature.
- $V_b$  terminal velocity of vapor slug.

$V_{b(\text{rel})}$	terminal velocity of vapor slug relative to liquid ahead of it.
$V$	velocity of steam inside tube.
$w$	tube wall thickness
$x$	vertical size of vapor slug.
$\dot{x}$	rate of change of vertical size with respect to time.
$y$	height of vapor slug above tank bottom.
$\alpha$	correlation constant defined by equation (7).
$\beta$	correlation constant defined by equation (7).
$\Gamma_c$	defined by equation (15).
	film thickness defined by equation (16).
	density of steam inside tube at $T_{\text{sat}}$ and $P$ .
$\rho_f$	density of saturated liquid at film temperature.
$\rho_g$	density of saturated vapor at film temperature.
	liquid-vapor interface surface tension.
$\mu$	viscosity of steam inside tube.
$\mu_f$	viscosity of liquid water at film temperature.
$\Delta T_B$	$= T_{\text{sv}} - T_B$
$\Delta T_i$	$= T_{\text{sv}} - T_{\text{si}}$
$\Delta P$	pressure difference to produce observed subcooling, see reference (7).